Multi-Wavelength Investigations of Solar Activity
Proceedings IAU Symposium No. 223, 2004
A.V. Stepanov, E.E. Benevolenskaya & A.G. Kosovichev, eds.

DOI: 10.1017/S1743921304005046

The long-term evolution of active regions, multi-wavelength flux and heating studies: observations and theory

P. Démoulin

Observatoire de Paris, LESIA, UMR 8109 (CNRS), F-92195 Meudon Cedex, France

Abstract.

Analyzing the long-term evolution of active regions (ARs) permits to quantify the link between their atmospheric emission (from optical to X-rays) and the magnetic field. Multi-wavelength studies provide the full story, and not just a snapshot, of the phenomena and they allow us analyze how the atmosphere changes as the field strength decreases (with the dispersion of the AR).

The evolution of the emitted flux in various wavelength ranges contains information on the heating mechanism(s) of the different atmospheric levels. I review what we can learn from such long-term (months) multi-wavelength observations, and compare the results to other solar and stellar studies.

1. Heating

As most cool stars, the Sun has a chromosphere and a corona. Since several decades, the outward increase of temperature in the stellar atmospheres has been attributed to an in situ heating. However, the precise mechanism(s) that heats stellar atmospheres is not known. Recently, several independent approaches converge to a coronal heating generated by stochastic buildup of energy, current layers and/or MHD turbulence (Mandrini *et al.* 2000, Schrijver & Aschwanden 2002, Démoulin *et al.* 2003). The origin of the chromospheric heating is less understood (Ulmschneider *et al.* 1991). A two-component heating mechanism is plausibly present in the chromosphere: an acoustic wave heating in the unmagnetized region and a magnetic heating in flux tubes (Cuntz *et al.* 1999). But this view is presently questioned, the heating of the chromosphere may be dominantly linked to MHD processes involving, partly unresolved, magnetic fields (Fontenla *et al.* 1999). The heating of the region in between the corona and the chromosphere, the transition region (TR), probably comes from the energy transferred from the corona.

The heat deposited in each atmospheric layer is related to the flux emitted from each layer. However, the link between the emitted flux and the deposited heat is not simple, in particular, because the energetics of the layers are coupled by different energy transport processes. From an observational point of view the emitted fluxes can be separated in two components: the basal and the excess fluxes (Rutten *et al.* 1991, Schrijver 1991). The basal and excess fluxes are usually interpreted as the flux coming from the non-magnetized and magnetized atmosphere, respectively. The basal flux is dominant in chromospheric lines and its importance decreases with increasing temperature, it has a small contribution to the total flux in TR lines and it is not detected in soft X-rays. The basal flux is independent of the rotation speed of the star, so it is thought to be independent of the observed magnetic field since the magnetic dynamo is generally linked to the stellar-rotation rate. Conversely, the excess flux increases with temperature and

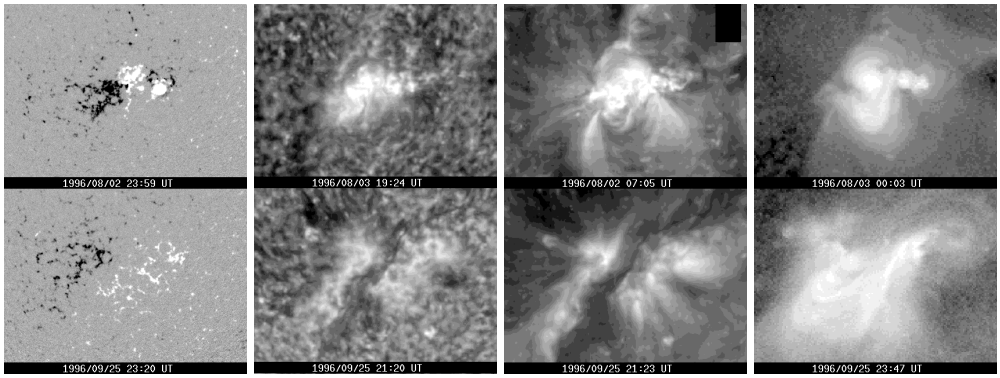

Figure 1. Evolution of AR 7978. From left to right: SoHO/MDI magnetic maps, SoHO/EIT He II 304 Å and Fe XII 195 Å images, Yohkoh/SXT images (co-aligned with the magnetic maps). The bottom row is observed two solar rotations after the first row.

it has a power-law dependence on the magnetic flux density. Such dependence contains information on the energy balance in the different layers.

2. Longterm evolution of an active region

In general, it is difficult to make a proper study of the long-term decay of an active region (AR) due to the nesting tendency of magnetic flux that leads to repeated flux emergence nearby or even within decaying ARs (Brouwer & Zwaan 1990, Harvey & Zwaan 1993). This is especially so during periods of high activity. Magnetic fields of neighbouring ARs interact, leading to an increased magnetic cancellation rate and shortened lifetime of the AR. A relatively undisturbed decay phase of ARs could only be studied around the solar minimum. Such was the case of AR 7978, which was the last major AR of cycle 22. In the period from August to October 1996, AR 7978 was nearly alone on the Sun (Oláh *et al.* 1999). Moreover, AR 7978 had a simple bipolar magnetic configuration, which was preserved through its long-term evolution. Thus, AR 7978 provided a unique opportunity to study the evolution of an isolated magnetic bipole, a basic configuration which is often used in models.

On 4 July 1996, AR 7978 emerged inside the dispersed remnant magnetic fields of a decayed AR. The total magnetic flux increased until the third rotation, while later on the sunspots disappeared. Then, the evolution of the photospheric field was mainly determined by magnetic diffusion and differential rotation (Fig. 1). The field spread over an ever increasing area and it was progressively transformed from a spot through a plage state into an enhanced network. This is the typical long-term evolution of isolated ARs (van Driel-Gesztelyi 1998, van Driel-Gesztelyi *et al.* 2003).

The chromospheric and transition region emission closely followed the evolution of the magnetic field. For example, the emitting facular area seen with in the 304 Å filter followed closely the dispersion of the photospheric field (Fig. 1). As the photospheric field became dispersed the intensity decreased. The spatial distribution of the emission in hotter lines ($\approx 1-2\times10^6$ K), is similar to the one in the 304 Å filter but it was also modified by the magnetic field expansion and reorganization with height. Hot and dense plasma filled a fraction of the magnetic flux tubes either fully (at earlier times of the AR) or partially (in particular in large scale loops where the gravitational scale height was smaller than the loop top height). At even higher temperatures ($\approx 2-5\times10^6$ K), more full loops were observed, while there was no longer emission located just above the

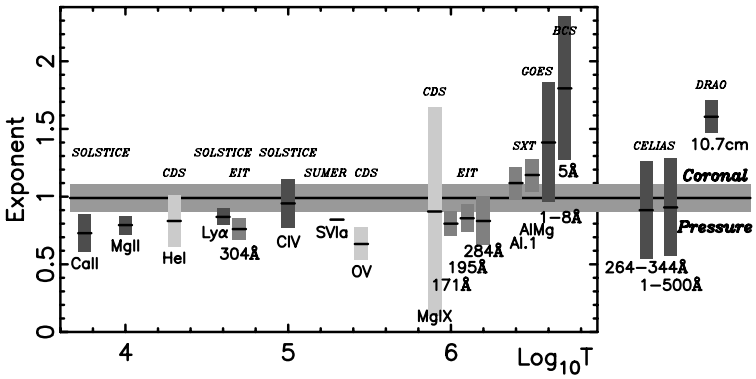

Figure 2. Ranges for the exponents, b, found for the power-law relations between the detected excess flux density and the magnetic flux density in different spectral domains, $\Delta F \propto \bar{B}^b$ (van Driel-Gesztelyi *et al.* 2004). The results are approximately ordered along the abscissa according to the mean temperature of the emitting plasma (except when the ranges overlap, e.g. in X-rays). Results at the extreme right, outside of the box, have such a broad wavelength (temperature) range that a mean temperature cannot be defined. The ordinate extension of the shaded regions represent the $\pm 3\sigma$ error range. The full-disk (stellar-like) measurements are dark shaded, while the spatially resolved measurements are light shaded, with the lightest shading for the spectrometers (CDS, SUMER). The horizontal grey band corresponds to the range of the exponent for the coronal plasma pressure. In the X-ray range, the exponents are corrected for the temperature dependence of the instrumental response function (Démoulin *et al.* 2004).

photospheric field concentrations (SXT images in Fig. 1). Instead, there was a diffuse emission which had both instrumental and physical (unresolved loops) origins.

Taking one set of data per rotation at each consecutive central meridian passage of the AR, outside the time of flares, van Driel-Gesztelyi *et al.* (2004) analyze multi-wavelength and multi-instrument data obtained from SoHO (MDI, EIT, CDS, SUMER and CELIAS/SEM), Yohkoh (BCS, SXT), GOES, SOLSTICE and 10.7 cm radio data from DRAO, Canada. From all these various data, they derive the mean radiative excess flux densities: ΔF = (flux - basal flux) per unit surface for each rotation. All the ΔF values are linked to the photospheric mean magnetic flux density, $\bar{B}$, by power laws: $\Delta F \propto \bar{B}^b$, and the exponent b depends on the formation temperature of the spectral lines involved (Fig. 2). For the soft X-rays detected by space-born instruments the dependence is almost quadratic ($b = 1.6 - 2.6$), while for the transition region and the chromosphere the dependence of the measured fluxes is more linear ($b = 0.7 - 1.$).

3. Coronal radiative fluxes

3.1. *Relationship with the magnetic flux*

Early works showed a nearly linear dependence of the solar X-ray flux density on the magnetic flux density: $F \propto B^{0.9\pm0.1}$ (Saar & Schrijver 1987, Schrijver *et al.* 1989). This linear relationship was corroborated by the results obtained using cool stars data. However, it is striking that, considering only the results found by those authors for the global Sun at minimum and maximum activity (see their Fig. 2), a quadratic dependence is present.

More recently, Fisher *et al.* (1998) found that the X-ray luminosity, $L_{\rm X}$ (total flux), of ARs correlates best with their total magnetic flux, $\Phi_{\rm tot}$: $L_{\rm X} \propto \Phi_{\rm tot}^{1.19\pm0.04}$. Moreover,

they find that this dependence explains all the other correlations found between L_X and several magnetic variables (like the total unsigned vertical current density or the total transverse field square). Pevtsov *et al.* (2003) extended the analysis to six main groups of data: quiet Sun, X-ray bright points, ARs, average Sun, and also dwarf and T-Tauri stars. When they analyzed each group separately they found power laws with exponents ranging from 0.9 to 2 (except for T-Tauri stars where no dependence is found). However, when all data are analyzed together they found $L_X \propto \Phi_{tot}^{1.15\pm0.05}$, a relation which extends the results of Fisher *et al.* over 12 orders of magnitudes in magnetic flux ! However, since an important natural correlation exists between L_X and Φ_{tot} via the spatial extension of the magnetic structure considered, it would be preferable to use intensive quantities (like F and $\bar{B}$), and not extensive quantities (like L_X and Φ_{tot}), to be sure that the approximate linear relationship obtained is not due to a proportionality of the extensive quantities with the magnetic area considered (and with relatively smaller variations of the intensive quantities).

Benevolenskaya *et al.* (2002) found a high correlation between the soft X-ray flux density of the corona (Yohkoh/SXT, AlMg filter) and the photospheric field (Kitt Peak magnetograms) from 1991 to 2001. They first constructed synoptic maps with 1^0 spatial resolution, that were afterwards averaged in longitude. They found that the soft X-ray flux density, F, follows a power-law with the averaged magnetic flux density, $\bar{B}$: $F \propto \bar{B}^b$. The exponent b has a solar cycle variation when $\bar{B}$ is above 8 G, b is higher during the declining phase (1.85 ± 0.02) than during the rising phase (1.64 ± 0.02). When the full range of field strengths was used, the exponent is slightly higher, ≈ 2, and almost independent of the activity.

3.2. *Why so different results ?*

The above results range from nearly linear to quadratic relationship. What are the main sources of these differences ? Of course the methods are different, but the main difference is the following. The measured X-ray fluxes are strongly affected by the instrumental response $R(T)$ because $R(T)$ is not peaked around a given temperature, but rather increases strongly with temperature. Correcting for this instrumental effect using the observed mean temperature, Démoulin *et al.* (2004) found that the scaling obtained for Yohkoh/BCS, Yohkoh/SXT and GOES data are basically the same ($\Delta F_{X-rays} \propto \bar{B}^{1.1-1.2}$, see Fig. 2). They are only slightly higher than the exponents found in the TR ! So during the long-term evolution of AR 7978, the ratio of emitted X-ray flux over emitted UV flux is only slightly decreasing. This is in agreement with the energy balance of quasi-static coronal loops, the coronal heating is compensated by two loss terms of comparable magnitudes: coronal radiation and downward transport to the TR, where the energy is then radiated (e.g. Vesecky *et al.* 1979).

The efect of $R(T)$ clarifies the difference between the exponents found in recent works. Benevolenskaya *et al.* found higher exponents, comparable to the ones found by van Driel-Gesztelyi *et al.* because the measured fluxes where not corrected for the instrumental response function $R(T)$ (flux unit is data number). In the study of Fisher *et al.* SXT data numbers are transformed to fluxes but with an assumed fixed temperature (3×10^6 K) so the temperature dependence of $R(T)$ was not taken into account. However, this is probably not so important in their study since they considered a set of ARs in the same evolutionary stage, where the temperature is likely to be similar and without important correlation with the measured fluxes (but it is still necessary to verify this statement). In the study of Pevtsov *et al.*, the temperature was estimated in most of their data groups, and $R(T)$ was taken into account. In conclusion, the response function dependence on temperature is the main source of the discrepancy between the exponents

found using X-ray data; but all of them are indeed compatible (or close to be) and this is remarkable since the methods used are so different.

3.3. *Cool stars*

It is also worth to compare with the results obtained for cool stars. As in the solar case, the observational results should first be corrected for the instrumental response function $R(T)$, which was not always done (see Piters *et al.*, 1997 for the effect of $R(T)$). When older measurements are included, usually a nearly quadratic relationship is found (e.g. Shi *et al.* 2002 found an exponent of 1.95 ± 0.14). But restricting to recent, so improved, measurements, Saar (1996,2001) found a nearly linear relationship instead (the exponents in the two studies are 0.95 and 1.0, respectively). So recent results on cool stars are in close agreement with the solar results. This clearly strengthens the importance of the relation between the emitted flux and the magnetic field since it is the main common conclusion of the different solar and stellar studies.

4. Transition-region radiative fluxes

4.1. *Relationship with the magnetic flux*

Schrijver (1990) was the first who related the flux density, $F_{\rm CIV}$ of the C IV line (observed with SMM-UVSP) to the photospheric magnetic flux density, B (from National Solar Observatory). He used three kinds of data: the slope of the distribution functions (or histograms) of $F_{\rm CIV}$ and B, the mean fluxes in quiet regions and ARs, as well as data from cool stars. He derived the dependence $\Delta F_{\rm C\ IV} \propto B^{0.74\pm0.05}$, when the basal flux was removed (Schrijver 1991).

Preś & Phillips (1999) analyzed the evolution of several bright points in quiet regions using the 195 Å filter of EIT. They showed that the luminosity, $L_{\rm UV}$, changed approximately in phase with the underlying magnetic flux $\Phi_{\rm tot}$. More precisely, they found $L_{\rm UV} \propto \Phi_{\rm tot}^b$ with an exponent b in the range [0.72,1.2] (excluding their case E which is only partially in their data region).

Ravindra & Venkatakrishnan (2003) analyzed the correlation between the He II (304 Å filter of EIT) network flux density, $F_{\rm He\ II}$, and the magnetic flux density, B (using both magnetograms from MDI and from the National Observatory of Kitt Peak). They showed that $F_{\rm He\ II}$ is well correlated, at the pixel-to-pixel level, both spatially and temporally with B. For $B > 10$ G they get a linear relationship between $F_{\rm He\ II}$ and B.

Fludra *et al.* (2002) studied 50 ARs with CDS, obtaining one measurement point for each AR. They find a power-law relationship between the spatially integrated line flux and the total magnetic flux, and obtain the following exponents: 0.8 for He I, 0.7 for O V, 0.7 for Mg X, and 1.2 for Fe XVI.

Fludra & Ireland (2003) analyzed the relationship between the CDS Fe XVI 360.76 Å line flux and the magnetic field from MDI magnetograms for 25 ARs. Assuming a power-law dependence $F \propto B^\delta$ of the line flux from individual loops on the magnetic flux density, B, at the loop footpoints, they derive an exponent $\delta = 1.3 \pm 0.3$.

The above results are broadly compatible with the results obtained from the longterm analysis of AR 7978 by van Driel-Gesztelyi *et al.* (2004): see Fig. 2. There is an intertwine of three types of instruments: imager with filters (EIT), imager with spectrograph (CDS, SUMER), and full disk spectrometer (SOLSTICE, CELIAS), but there is no systematic shift of the exponents between these different instruments.

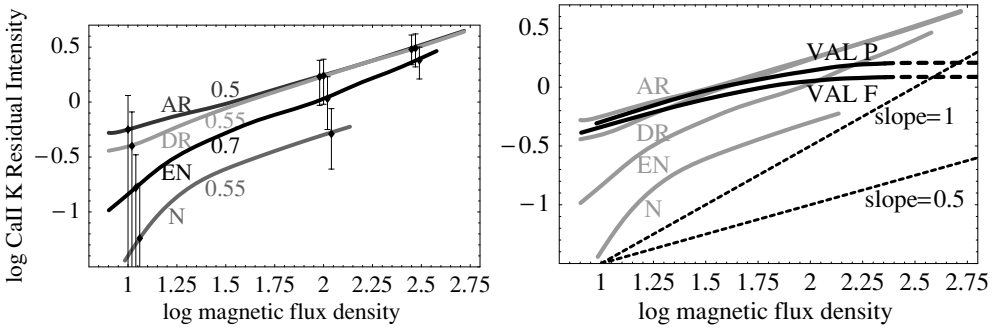

Figure 3. Left panel: Log-log plots of the Ca II K residual intensity, δK (nearly proportional to the Ca II K core/wing excess flux ratio) versus magnetic flux density, B, summarising the results of Harvey and White (1999). The continuous curves are for four structures: active region plage (AR), decaying active regions (DR), enhanced network (EN) and network (N). The nearly straight part (at high field value) are fitted with a power-law $\delta K \propto B^e$, and the exponent e is indicated on the right hand side of the symbols. There is indeed a large overlap between these structures because of a large intrinsic dispersion as indicated by the "error bars" set for $\pm 1\sigma$. **Right panel**: Comparison of the observational results of Harvey and White (1999) with the theoretical results of Solanki *et al.* (1991). The black continuous lines summarize the results of Solanki *et al.* for a photospheric field $B_0 = 1500$ G; this B_0 value is used to convert their filling factor to magnetic flux density. The magnetized atmosphere is modelled with a given VAL model which is kept for the entire flux density range. Their flux result for a null filling factor (non-magnetized atmosphere) is used to estimate and remove the basal flux. A constant shift in the ordinate is introduced to convert line core to wing intensity ratio of Solanki *et al.* to the residual intensity of Harvey and White.

4.2. *Interpretation*

There are three possible sources of the UV flux: small scale cool loops (Athay 1985, Feldman & Laming 1994), UV loops and transition region emission of X-ray loops (e.g. Martens *et al.* 2000). The recent, spatially better resolved, observations have put serious limits on the spatial extension and emissivity of the hypothetical cool loops both in the quiet Sun and in ARs (Griffiths *et al.* 2000, Vourlidas *et al.* 2000). The physics of UV loops is presently largely debated (Reale & Peres 2000, Aschwanden *et al.* 2000, Warren *et al.* 2003). In such open context concerning the physics involved, it is difficult to isolate the emission of UV loops since we can only rely on observations. Indeed, it is very difficult to isolate the total emission of UV loops from the TR emission of X-ray loops. UV loops could plausibly provide a significant, but unknown, contribution to the UV emission.

The physics involved in the transition region of X-ray loops is the most understood. At least, four mechanisms can transport heat in the transition region (TR). They are the classical thermal conduction by electrons (Spitzer 1962, Lie-Svendsen *et al.* 1999), the enhanced conduction by turbulence (Cally 1990), the ambipolar diffusion of ions and neutral atoms (Fontenla *et al.* 1990), and the transport by plasma flows (Chae *et al.* 1997). Démoulin *et al.* (2004) concluded that these four principal mechanisms of energy transport give theoretical scaling laws compatible with those deduced from the observations (Fig. 2).

5. Chromospheric radiative fluxes

5.1. *Relationship with the magnetic flux*

Schrijver *et al.* (1989) analyzed the distribution of the Ca II K core/wing flux ratio, $\Delta F_{\rm Ca\ II}$, versus magnetic flux density, B, in ARs. They found: $\Delta F_{\rm Ca\ II} \propto \bar{B}^{0.6\pm0.1}$ when

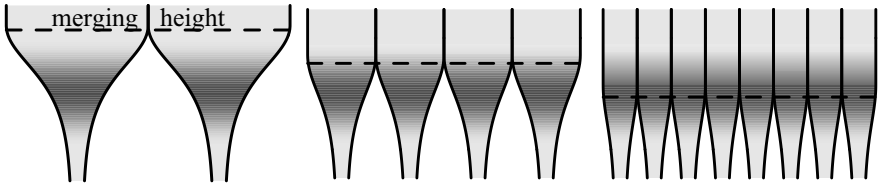

Figure 4. Schematic representation of models of the emission of chromospheric lines outlining the main effects of a changing magnetic filling factor. The emitting layer is simply represented with a darker region. Present observations are not able to resolve the flux tubes, but rather measure the mean excess flux, $\Delta\bar{F}$, and the mean magnetic flux $\bar{B}$ (say, from all the flux tubes shown in each frame). The same atmosphere is kept as $\bar{B}$ increases from the left to the right. It corresponds to an increase of $\Delta\bar{F}$ which saturates as the magnetic flux tubes get into contact in the emission region (right frame). This summarizes the main result of Solanki *et al.* (1991, see Fig. 3).

the basal flux was removed (Schrijver 1991). Harvey & White (1999) extended previous work with a meticulous analysis of the Ca II emission. They defined the Ca II K residual intensity, δK, as the intensity from the core of the Ca II K removing the quiet Sun value (and normalizing it to the mean quiet Sun value). They used three different instruments which integrate the line core over different spectral windows; they found nearly the same results for the three sets of data. Their results can be summarized with well defined power laws between δK and the local photospheric magnetic flux density, B, when B was large enough (typically 20-40 G, see their Table 4). They found $\delta K \propto B^{0.6\pm0.1}$ (Fig. 3). This is in agreement with Schrijver *et al.* (1989), so indeed, as expected from the definitions, the residual intensity, δK, is proportional to the Ca II K core/wing flux ratio, $\Delta F_{\mathrm{Ca\ II}}$.

5.2. *Models*

The expansion of magnetic flux tubes could be at the origin of the link between the excess chromospheric flux and the magnetic flux density (Fig. 4). Solanki *et al.* (1991) computed the flux of the Ca II K line using a hydromagnetic model of an expanding flux tube. The atmosphere of the magnetic and non-magnetic regions was selected from semiempirical VAL models (Vernazza *et al.* 1981) and it was considered independent of the surface filling factor, f_m, of the photospheric flux tubes. The key point is that the extension of the magnetized atmosphere depends on f_m (Fig. 4). It implies that the emitted flux, $\bar{F}$, is a function of f_m and so of the magnetic flux density, $\bar{B}$ (as observed without resolving the flux tubes). Both the emitting magnetized region and $\bar{F}$ increase with $\bar{B}$ (while the merging height decreases). However, for $\bar{B}$ large enough, the merging height, h_m, becomes lower than the bottom height of the region where the line is formed; then, the emitted flux saturates at a fixed value (Fig. 3, right panel).

Can the above variable contribution of the magnetized and non-magnetized regions explain the observations ? Indeed, the results of Schrijver (1993), Harvey & White (1999) and van Driel-Gesztelyi *et al.* (2004) show a power law which is especially well defined for the high flux density value while the results of Solanki *et al.* show an intrinsic saturation of the flux. Because it is intrinsic to the physics involved, this saturation extends indeed to larger flux densities (dashed line in the right panel of Fig. 3) than their numerical computation range (continuous line). Then, keeping the same model for the magnetized atmosphere (independent of $\bar{B}$), the change of the magnetized region with the magnetic filling factor f_m cannot explain the observations.

The chromospheric emission is not simply linked to the energy deposited in the formation region since there is a strong link to the radiation coming from photospheric and neighbour chromospheric layers. Building a full model of the chromosphere is still a

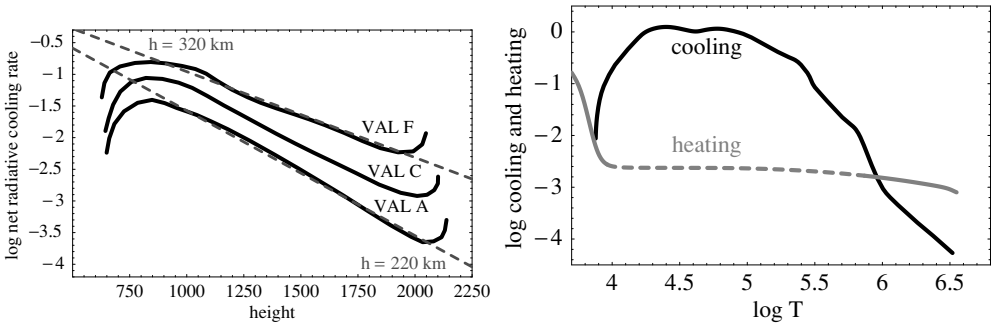

Figure 5. Left panel: Mean total radiative cooling rate (continuous lines) as deduced from the VAL models of the chromosphere (adapted from Avrett 1981). The scale height h is deduced in the region having an exponential decrease. **Right panel**: Schematic log-log plot of the radiative cooling, $N_e^2\Lambda$, and heating, H, per unit volume and time present in the solar atmosphere (in ergs cm^{-3}s^{-1}). The plot is done for a constant pressure of ≈ 1 dyn cm^{-2}. The cooling function is taken from Chae, Yun & Poland (1997). In the chromosphere, H follows the results of Avrett (1981), while in the corona H has the typical value deduced from observations (e.g. Martens, Kankelborg & Berger, 2000). In the chromosphere the emitted net radiation balances the local heating, while this is not so in the TR and the corona, where the energy transport (e.g. by thermal conduction) accounts for the difference. There is no observational constraint for the heating rate in the TR (a fact coherent with theory since the heating is negligible in the energy budget). The dashed line indicates that the chromospheric and coronal heating probably extends into the TR and it emphasizes that there is plausibly a unique heating mechanism of the magnetized regions.

great challenge and present understanding of the chromosphere rather rely on the semi-empirical FAL models of Fontenla *et al.* (1999). The flux emitted in the Ca H & K and Mg h & k lines is computed with these models using the software PANDORA (Démoulin *et al.*, 2004). The model FAL A, obtained for faint supergranular cell interior, is used to remove the basal flux from models C, F and P (for average supergranular cell interior, bright network or faint plage, and bright plage, respectively) to get the excess flux ΔF. The plasma pressure P, is obtained from the FAL models at $T = 10^5$ K. Log-log plots of $F(P)$ are only very approximately represented by a power law, moreover with an exponent which is changing with the line considered. However, the log-log plots of $\Delta F(P)$ are almost linear with an exponent close to one ([0.87,1.16]) for the four lines. This result is close to the results summarized in Figs. 2 and 3, but with slightly too high exponents. Démoulin *et al.* (2004) conclude that the emission of the upper chromosphere is a function of the magnetic flux density, $\bar{B}$, not only because of the evolution of the flux tube shape with $\bar{B}$, but dominantly because the magnetized plasma is heated differently (so that, as $\bar{B}$ decreases the magnetized atmosphere should be described by a "cooler" VAL/FAL model).

6. Conclusion

We have learned that the magnetic field is not only a strong structuring agent of the solar atmosphere, but also that it defines its main properties (such as pressure and temperature). There is plausibly a unique heating mechanism in the magnetized part that heats both the upper chromosphere and the corona (Fig. 5). The heating rate scales approximately with the magnetic field to the second power (transforming all the parameter dependence to the magnetic one). In the intermediate layer, the TR, this heating mechanism could well be at work, but the presence of such high radiative losses makes this

heating input unimportant for the TR physics. Finally, taking into account the observed universality of the flux-flux relations (power laws between fluxes from the optical to the X-ray range), this physical scenario is expected to extend to cool stars.

Acknowledgements

I thank Lidia van Driel-Gesztelyi for her help in the improvement of the manuscript.

References

Aschwanden, M. J., Nightingale, R. W., & Alexander, D. 2000, ApJ, 541, 1059
Athay, R. G. 1985, Solar Phys., 100, 257
Avrett, E. H. 1981, in NATO ASIC Proc. 68: Solar Phenomena in Stars and Stellar Systems, 173
Benevolenskaya, E. E., Kosovichev, A. G., Lemen, J. R., Scherrer, P. H., & Slater, G. L. 2002, ApJ, 571, L181
Brouwer, M.P. & Zwaan, C. 1990, Solar Phys., 129, 221
Cally, P. S. 1990, ApJ, 355, 693
Chae, J., Yun, H. S., & Poland, A. I. 1997, ApJ, 480, 817
Cuntz, M., Rammacher, W., Ulmschneider, P., Musielak, Z. E., & Saar, S. H. 1999, ApJ, 522, 1053
Démoulin, P., van Driel-Gesztelyi, L., Mandrini, C. H., Klimchuk, J. A., & Harra, L. 2003, ApJ, 586, 592
Démoulin, P., van Driel-Gesztelyi, L., Mandrini, C.H., Mauas, P., de Groof, A. 2004, Solar Phys., submitted
Feldman, U. & Laming, J. M. 1994, ApJ, 434, 370
Fisher, G. H., Longcope, D. W., Metcalf, T. R., & Pevtsov, A. A. 1998, ApJ, 508, 885
Fludra, A. & Ireland, J. 2003, A&A, 398, 297
Fludra, A., Ireland, J., del Zanna, G. & Thompson, W. T. 2002, Adv. Space Res., 29, 3, 361
Fontenla, J. M., Avrett, E. H., & Loeser, R. 1990, ApJ, 355, 700
Fontenla, J., White, O. R., Fox, P. A., Avrett, E. H., & Kurucz, R. L. 1999, ApJ, 518, 480
Griffiths, N. W., Fisher, G. H., Woods, D. T., Acton, L. W., & Siegmund, O. H. W. 2000, ApJ, 537, 481
Harvey, K. L. & White, O. R. 1999, ApJ, 515, 812
Harvey, K.L. & Zwaan, C. 1993, Solar Phys., 148, 85
Lie-Svendsen, Ø., Holzer, T. E., & Leer, E. 1999, ApJ, 525, 1056
Mandrini, C. H., Démoulin, P., & Klimchuk, J. A. 2000, ApJ, 530, 999
Martens, P. C. H., Kankelborg, C. C., & Berger, T. E. 2000, ApJ, 537, 471
Oláh, K., van Driel-Gesztelyi L., Kővári, Zs. & Bartus, J. 1999, A&A, 344, 163
Pevtsov, A. A., Fisher, G. H., Acton, L., *et al.* 2003, ApJ , 598, 1387
Piters, A. J. M., Schrijver, C. J., Schmitt, J. H. M. M., *et al.* 1997, A&A, 325, 1115
Preś, P. & Phillips, K. J. H. 1999, ApJ, 510, L73
Ravindra, B. & Venkatakrishnan, P. 2003, Solar Physics, 214, 267
Reale, F. & Peres, G. 2000, ApJ, 528, L45
Rutten, R. G. M., Schrijver, C. J., Lemmens, A. F. P., & Zwaan, C. 1991, A&A, 252, 203
Saar, S. H. 1996, in IAU Symp. 176: Stellar Surface Structure, 237
Saar, S. H. 2001, in ASP Conf. Ser. 223: 11th Cambridge Workshop on Cool Stars, Stellar Systems and the Sun, 292
Saar, S.H. & Schrijver, C.J. 1987, in Cool Stars, Stellar Systems, and the Sun, e.d. L. linsky and R. E. Stencel, New York, Springer-Verlag, p. 38.
Schrijver, C. J. 1990, A&A, 234, 315
Schrijver, C. J. 1991, in Mechanisms of Chromospheric and Coronal Heating. Editors, P. Ulmschneider, E.R. Priest, R. Rosner; Publisher, Springer-Verlag, Berlin, Germany, 257
Schrijver, C. J. 1993, A&A, 269, 395
Schrijver, C. J. & Aschwanden, M. J. 2002, ApJ, 566, 1147

Schrijver, C.J., Coté, J., Zwaan, C. & Saar, S.H. 1989, ApJ, 337, 964
Shi, J. R., Zhao, G., & Zhao, Y. 2002, Ap&SS, 282, 477
Solanki, S. K., Steiner, O., & Uitenbroeck, H. 1991, A&A, 250, 220
Spitzer, L. 1962, Physics of Ionized Gases (Interscience, New York)
Ulmschneider, P., Priest, E. R., & Rosner, R., eds. 1991, Mechanisms of Chromospheric and Coronal Heating, 328
van Driel-Gesztelyi, L. 1998, in *Three dimensional structure of solar active regions*, Proc. 2nd. ASPE, C. Alissandrakis, B. Schmieder (eds.), Astron. Soc. Pac. C.S., 155, 202.
van Driel-Gesztelyi, L., Démoulin, P., Mandrini, C. H., Harra, L., & Klimchuk, J. A. 2003, ApJ, 586, 579
van Driel-Gesztelyi, L., Démoulin, P., Oláh, K., *et al.* 2004, Solar Physics, submitted
Vernazza, J. E., Avrett, E. H., & Loeser, R. 1981, ApJs, 45, 635
Vesecky, J. F., Antiochos, S. K., & Underwood, J. H. 1979, ApJ, 233, 987
Vourlidas, A., Klimchuk, J. A., Korendyke, C. M., Tarbell, T. D., & Handy, B. N. 2001, ApJ, 563, 374
Warren, H. P., Winebarger, A. R., & Mariska, J. T. 2003, ApJ, 593, 1174